ISBN: 978-3-95450-253-0 ISSN: 2673-5571 doi:10.18429/JACoW-HB2023-WEC4I2

DEVELOPMENT OF DUAL-HARMONIC RF SYSTEM FOR CSNS-II*

Xiao Li†, Bin Wu, Jian Wu, Xiang Li, Yang Liu, Wei Long, Chunlin Zhang
Institute of High Energy Physics, Chinese Academy of Science, Beijing, China

Abstract

The upgrade of the China Spallation Neutron Source (CSNS-II) encompasses the development of a dual harmonic RF system for the Rapid Cycling Synchrotron (RCS). The objective of this system is to achieve a maximum second harmonic voltage of 100 kV. To meet this requirement, a high gradient cavity is being used in place of the traditional ferrite loaded cavity. Magnetic alloy (MA) loaded cavities, which can attain very high field gradients, have demonstrated their suitability for high-intensity proton synchrotrons. As a result, designing an RF system with MA-loaded cavities has emerged as a primary focus. Over the past decade, substantial advancements have been made in the development of MA-loaded cavities at CSNS. This paper provides an overview of the RF system that incorporates the MA-loaded cavity and presents the high-power test results of the system.

INTRODUCTION

The China Spallation Neutron Source (CSNS) is advancing into its upgrade phase (CSNS-II), targeting a higher beam power up to 500 kW. The key parameters of CSNS-II can be found in Table 1. The most important thing for the transverse and longitudinal beam dynamics is to address the strong space charge effect arising from the higher beam intensity. To counteract this, the dual-harmonic acceleration mechanism [1,2], which has already demonstrated its efficacy in mitigating the space charge effect, is slated for introduction. Given the limited tunnel space in Rapid Cycling Synchrotron (RCS), only a high-gradient cavity can fulfill the needs for the second harmonic voltage. Consequently, ferrite-loaded cavities, constrained by their low saturation flux density, fall short in comparison.

MA-loaded cavities, celebrated for their standout saturation flux density and permeability [3,4], emerge as the top choice for high-gradient applications. Their low Q-value and broad bandwidth further position them as uniquely capable of providing both fundamental frequency and second harmonic voltages without the necessity of a tuning loop. Over the past decade, extensive advancements have been made in the development of MA-loaded cavities at CSNS. Concurrently, the power supply and the low-level RF (LLRF) control systems have seen considerable development.

In this paper, we provide an overview of the RF system, including the MA-loaded cavity, RF amplifiers, and the LLRF system, and present the test results from high-power tests.

* Work supported by the funds of National Natural Science Foundation of China (Fund No: 11875270, U1832210, 12205317), Youth Innovation Promotion Association CAS (2018015). Guangdong Basic and Applied Basic Research Foundation (2019B1515120046).
† email address: lixiao@ihep.ac.cn

Table 1: Key Parameters of the CSNS-II

Linac end energy	300 MeV
RCS extraction energy	1.6 GeV
Beam power	500 kW
RF cavities	8 (1^{st}) + 3 (2^{nd})
RF voltages	175 kV (1^{st})) + 100 kV (2^{nd})
Number of bunches	2
Number of protons	7.80×10^{13} ppp

OVERVIEW OF THE RF SYSTEM

MA-loaded Cavity

The MA-loaded cavity is composed of three λ/4 double-resonators, each linked by three accelerating gaps, spanning a total length of 1.8 m. These resonators function as water tanks filled with MA cores. Tanks on the same side of the gaps are interconnected in parallel. A visual representation of this configuration can be found in Fig. 1.

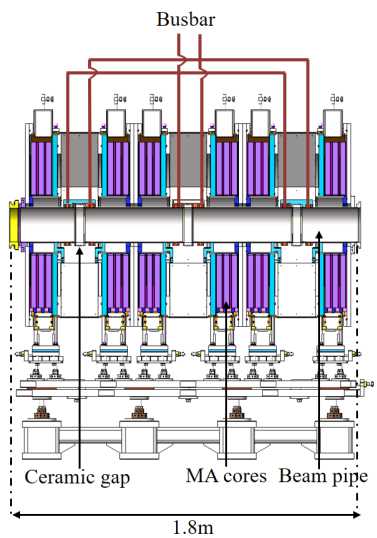

Figure 1: Schematic of the MA-loaded cavity.

The cavity incorporates a compact gap structure, engineered for robust voltage tolerance. It boasts a toroid constructed from alumina micro-powder, with stainless steel pipes embedded into the ceramic. This design minimizes the electric field exposure on the ceramic's surface and guarantees quick beam transit in the vacuum, facilitating efficient beam acceleration. To enhance the Q-value and amplify the operational prowess of the amplifier, two air inductors are aligned in parallel to the cavity. The impedance of the MA-loaded cavity, equipped with a 20 μH air inductor, is depicted in Fig. 2.

ISBN: 978-3-95450-253-0 ISSN: 2673-5571 doi:10.18429/JACoW-HB2023-WEC4I2

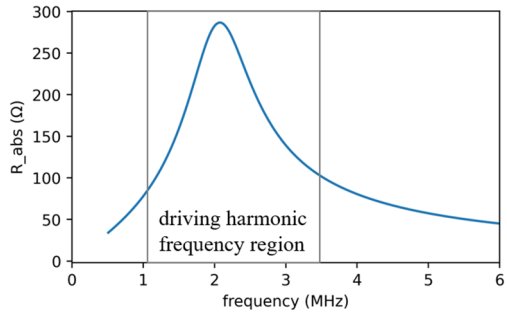

Figure 2: The impedance of the MA-loaded cavity with a 20 µH air inductor installed.

Two-stages RF Amplifiers

To achieve the high gradient demanded by the compact cavity design, we utilize a two-stage amplifier configuration. The pre-amplification phase employs a solid-state amplifier (SSA) with an 8 MHz bandwidth. Owing to the exceptional stability, efficiency, and cost benefits of tetrode tubes, and their capability to supply power on the order of hundreds of kilowatts across a broad frequency range [5], the final-stage amplification features two high-power tetrode tubes in a push-pull configuration. Figure 3 shows both the SSA and the tetrode tube amplifiers.

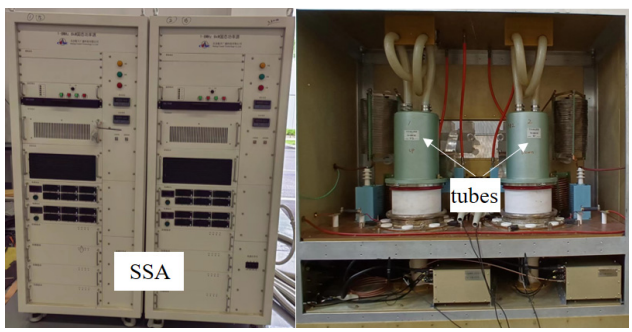

Figure 3: The SSA and tetrode tube amplifiers.

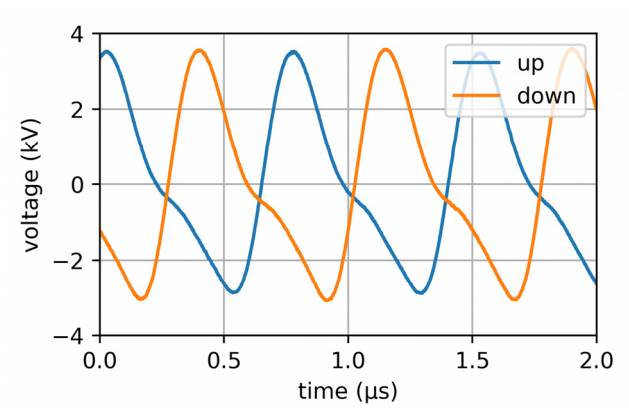

Figure 4: The cavity voltage exhibits significant harmonic content due to the non-linearity of the amplifiers.

An impedance matching system is in place to ensure optimal signal transmission between the SSA and tetrode tubes. These tubes are operated in the AB1 class for high efficiency. However, the inherent non-linearity of amplifiers combined with the wideband impedance of the cavity gives rise to pronounced higher harmonics, as visualized in Fig. 4. Addressing these unwanted harmonics necessitates the control algorithm implementation in a low-level RF (LLRF) control system.

LLRF Control System

The LLRF system is mainly response for monitoring and regulating the RF field in the cavities according to the voltage program. All the detection and control techniques such as demodulation and proportional-integral-derivative (PID) algorithm are implemented in a field-programmable gate array (FPGA) as shown in Fig. 5. The FPGA is equipped with four Analog-to-Digital Converters (ADCs), each capable of a maximum sampling rate of 120 MHz. One digital signal processor (DSP) is also equipped for data processing. To provide ample storage for essential data, the board is outfitted with two 512 MB memories. This storage capacity enables the recording of valuable data for commissioning, monitoring, and analysis purposes.

In terms of voltage regulation for the MA-loaded cavity, precise control of the driving harmonic is essential to align with the voltage program, while any undesired higher harmonics must be effectively compensated for. Therefore, a multi-harmonic feedback control algorithm has been developed. The simplified block diagram of control system is shown in Fig. 6. It is very simple since it does not require an active tuning loop.

Figure 5: LLRF control system.

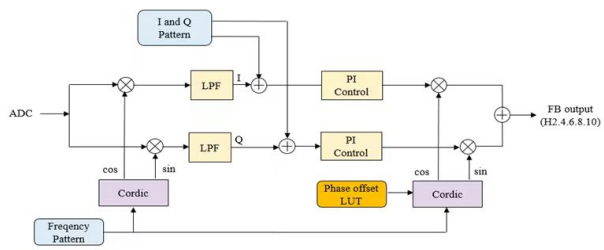

Figure 6: The simplified block diagram of the multi-harmonic feedback control.

TEST RESULTS

Field Gradient Test

The tested voltage pattern of (H=4) has a parabolic shape and operates over a period of 6 ms. The cavity field was gauged using two voltage monitors connected to an oscilloscope. The MA-loaded cavity showcased exemplary performance, achieving an impressive synthetic peak voltage of 90 kV (30 kV per gap) without any gap flashover incidents. This equates to a field gradient of approximately 50

ISBN: 978-3-95450-253-0 ISSN: 2673-5571 doi:10.18429/JACoW-HB2023-WEC4I2

kV/m, which is almost double the gradient attained by the ferrite-loaded cavity. The waveform captured by the oscilloscope is displayed in Fig. 7. It's evident from the two bottom waveforms, representing the control grid voltage, that there is significant distortion. This distortion arises from the screen grid overcurrent in the tetrode tube, limiting the possibility of reaching even higher field gradients. Nonetheless, it's important to highlight that by upgrading the anode power supply, higher field gradients could potentially be achieved, paving the way for enhanced performance in future endeavours.

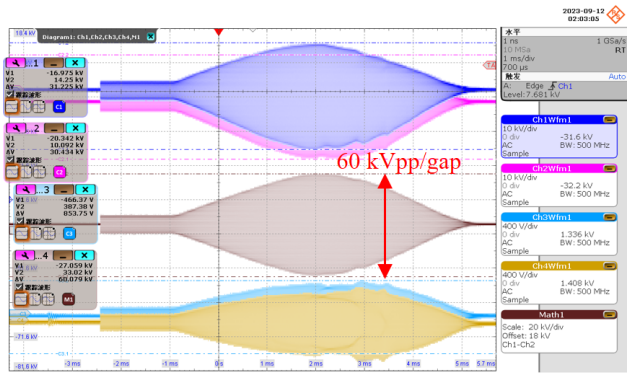

Figure 7: The measured waveform of cavity voltage of 60 kVpp of each gap.

LLRF Control System Performance Test

The LLRF control system not only plays a crucial role in compensating for unwanted higher harmonics but also ensures the stability of both amplitude and phase for the driving harmonic. In Fig. 8, the upper graph displays the cavity waveform when only feedback for the driving harmonic (H=4) is applied. However, the main higher harmonic observed is the 2nd harmonic (H=8), with a few components of the 3rd harmonic. By implementing feedback controls for the higher harmonics with setpoints of (0, 0), the components of these higher harmonics are effectively reduced, as depicted in the bottom graph of Fig. 8. Consequently, the cavity voltage exhibits a nearly pure sine signal, indicating the successful functioning of the multi-feedback control system.

It is important to note that closing the feedback loops for the higher harmonics can potentially impact the control performance of the driving harmonic due to slight coupling caused by amplifier nonlinearity. However, thanks to the application of adaptive feedforward control [6] for the driving harmonic, the control performance is significantly enhanced. The amplitude and phase control performance, as shown in Fig. 9, are well maintained below ±1.0% and ±1°, respectively. These results successfully meet the design requirements of the RF system.

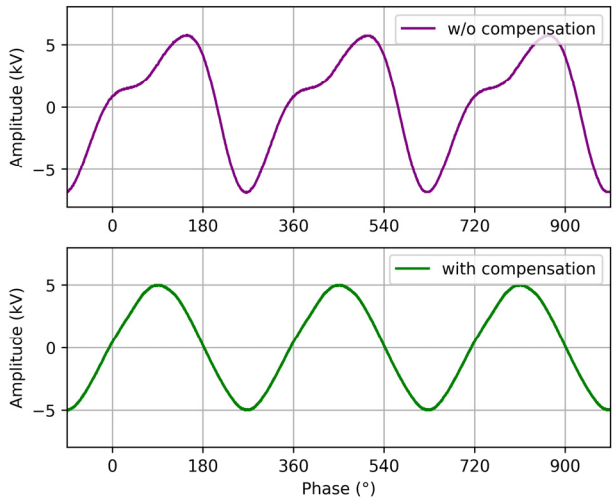

Figure 8: The cavity voltage waveform (up) without and (down) with higher harmonics compensation.

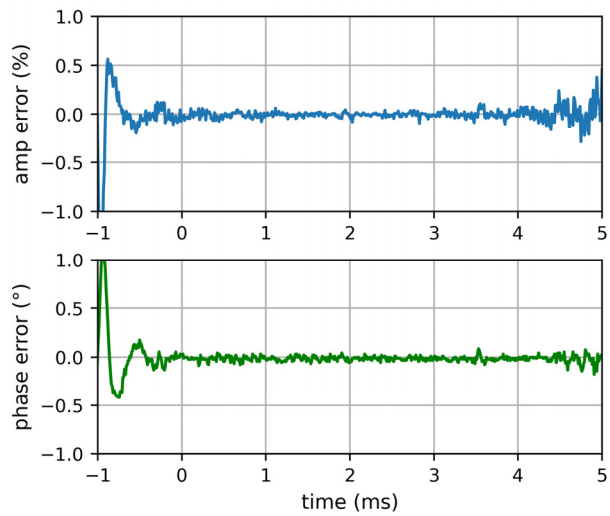

Figure 9: The (up) amplitude and (phase) control performance of the driving harmonic by LLRF.

CONCLUSION

A prototype of the MA-loaded cavity has been successfully developed to enable dual harmonic acceleration in the CSNS-II RCS. The experimental results of achieving a gradient of 50 kV/m not only demonstrate the high-gradient characteristics of the magnet alloy cavity but also validate the excellent output capability of the power source system. The significant harmonic distortion due to the wideband nature of the cavity and the dynamic-tube characteristics is effectively mitigated by a multi-harmonic feedback control algorithm in LLRF system. Besides, the stability of both the amplitude and phase of the driving harmonic has been reliably maintained. These achievements are significant and provide a solid foundation for the future upgradation of the CSNS.

ISBN: 978-3-95450-253-0 ISSN: 2673-5571 doi:10.18429/JACoW-HB2023-WEC4I2

REFERENCES

[1] J. F. Chen and J. Y. Tang, "Studies of dual-harmonic acceleration at CSNS", *Chinese Phys. C*, vol. 34, p. 1643, 2010. doi:10.1088/1674-1137/34/10/018

[2] H. Liu and S. Wang, "Longitudinal beam dynamic design of 500 kW beam power upgrade for CSNS-II RCS", *Radiat. Detect. Technol. Methods*, vol. 6, pp. 339–348, 2022. doi:10.1007/s41605-022-00325-5

[3] K. Suzuki, A. Makino, A. Inoue, *et al*., "Soft magnetic properties of nanocrystalline bcc Fe-Zr-B and Fe-M-B-Cu (M=transition metal) alloys with high saturation magnetization". *J. Appl. Phys*., vol. 70, pp. 6232–6237, 1991. doi:10.1063/1.350006

[4] B. Wu, X. Li, Z. Li, *et al*., ``Development of a large nanocrystalline soft magnetic alloy core with high μQf products for CSNS-II", *Nucl. Sci. Tech*., vol. 33, pp. 1–10, 2022. doi:10.1007/s41365-022-01087-x

[5] S. K. Thakur, "Design and performance of high voltage power supply with crowbar protection for 3-Φ high power RF amplifier system of cyclotron", *J. Instrum.*, vol. 11, p. T07004, 2016. doi:10.1088/1748-0221/11/07/T07004

[6] X. Li, H. Sun, C.L. Zhang *et al*., "Design of rapid tuning system for a ferrite-loaded cavity", *Radiat. Detect. Technol. Methods*, vol. 5, pp. 324–331, 2021. doi:10.1007/s41605-021-00255-8